Inorganica Chimica Acta, 198–200 (1992) 469–481

New trinuclear and hexanuclear ruthenium clusters derived from the reaction of $[Ru_3(CO)_{12}]$ with phenylphosphine or cyclohexylphosphine

Antony J. Deeming*, Simon Doherty and Nicholas I. Powell
Department of Chemistry, University College London, 20 Gordon Street, London WC1H 0AJ (UK)

Abstract

The reaction of $[Ru_3(CO)_{12}]$ with RPH_2 (R = phenyl or cyclohexyl) has been re-examined and the involvement of the trinuclear clusters $[Ru_3(\mu\text{-H})(\mu\text{-PHR})(CO)_{10}]$, $[Ru_3H_2(\mu_3\text{-PR})(CO)_9]$, $[Ru_3H_2(\mu_3\text{-PR})(CO)_8(PH_2R)]$ and $[Ru_3H_2(\mu\text{-PHR})_2(CO)_8]$ in the formation of the bis-capped compound $[Ru_3(\mu_3\text{-PR})_2(CO)_9]$ has been explored. The single-crystal X-ray structures of $[Ru_3(\mu\text{-H})_2(\mu_3\text{-PPh})(CO)_8(PH_2Ph)]$ and $[Ru_3(\mu\text{-H})(\mu\text{-PHPh})_3(CO)_7]$ are presented. The latter compound was obtained as a single isomer whereas there are four isomers present in solutions of the PHCy analogue (Cy = cyclohexyl). In an unsuccessful attempt to hydrogenate $[Ru_3(\mu_3\text{-PR})_2(CO)_9]$ to reform one of the isomers, $[Ru_3H_2(\mu\text{-PHR})_2(CO)_8]$ or $[Ru_3H_2(\mu_3\text{-PR})(CO)_8(PH_2R)]$, we obtained instead a mixture of the known compound $[Ru_6(\mu_3\text{-PR})_2(\mu_4\text{-PR})_2(CO)_{12}]$ and the hydrogenated form of this, $[Ru_6H_2(\mu_3\text{-PR})_2(\mu_4\text{-PR})_2(CO)_{12}]$. The structures of these hexanuclear clusters are related, both being based on distorted trigonal prismatic Ru_6 arrangements, but the distortions are very different and the average Ru–Ru distances in the 90-valence electron dihydride are longer than in the 88-valence electron non-hydride compound. We have identified a restricted rotation about the P–Ph bonds for the μ_4-ligands but not the μ_3-ligands which is interpreted in terms of clashes of the *ortho*-phenyl hydrogen atoms with CO ligands.

Introduction

Phenylphosphine reacts with $[Ru_3(CO)_{12}]$ in refluxing hexane to give initially the complexes $[Ru_3H(\mu\text{-PHPh})(CO)_{10}]$ and $[Ru_3H_2(\mu_3\text{-PPh})(CO)_9]$ [1]; the crystal structures of these compounds and the osmium analogues have been determined [1, 2]. The reaction proceeds further to give $[Ru_3H_2(\mu_3\text{-PPh})(CO)_8(PH_2Ph)]$ and an isomer of $[Ru_3H_2(\mu_3\text{-PPh})(CO)_9]$ is also formed by orthometallation of the phenyl ring: $[Ru_3H_2(\mu_3\text{-PHC}_6H_4)(CO)_9]$ [1]. These isomers correspond directly to the aniline derivatives $[Os_3H_2(\mu_3\text{-NPh})(CO)_9]$ and $[Os_3H_2(\mu_3\text{-NHC}_6H_4)(CO)_9]$ which we described some years ago [3, 4]. Carrying out the reaction between $[Ru_3(CO)_{12}]$ and phenylphosphine at higher temperatures in refluxing toluene led to $[Ru_3(\mu_3\text{-PPh})_2(CO)_9]$ by loss of H_2 and to a series of higher nuclearity clusters containing phenylphosphinidene (PPh) ligands including $[Ru_4(PPh)(CO)_{10}]$, $[Ru_5(PPh)(CO)_{15}]$, $[Ru_6(PPh)_4(CO)_{12}]$ and $[Ru_6(PPh)_5(CO)_{12}]$ [5, 6]. Some of these compounds can also be obtained by P–C bond cleavage of diphenylphosphine. For example, $[Ru_6(PPh)_4(CO)_{12}]$ as well as $[Ru_7(PPh)_2(CO)_{18}]$ [7, 8] and a series of PPh_2 clusters were obtained from the reaction of $[Ru_3(CO)_{12}]$ with diphenylphosphine [7–9].

In this study we have re-examined some of the chemistry of PH_2Ph with $[Ru_3(CO)_{12}]$ and the interconnection between the trinuclear products on route to the dehydrogenation product $[Ru_3(PPh)_2(CO)_9]$ and in the course of this we examined the isomeric forms of $[Ru_3H_2(PHPh)_2(CO)_8]$ and $[Ru_3H(PHPh)_3(CO)_7]$ and determined the crystal structures of $[Ru_3H_2(PPh)(CO)_8(PH_2Ph)]$ and of one isomer of $[Ru_3H(PHPh)_3(CO)_7]$. We attempted to rehydrogenate the cluster $[Ru_3(PPh)_2(CO)_9]$ to reform the trinuclear clusters containing a higher hydrogen content but instead obtained the new hexanuclear cluster $[Ru_6H_2(PPh)_4(CO)_{12}]$, the structure of which is compared with that of the known structure of $[Ru_6(PPh)_4(CO)_{12}]$ which was also obtained from this reaction. These compounds are structurally related but show interesting differences as a result of the different electron counts (90 versus 88 electrons). Finally we have identified fluxionality based on a severely restricted rotation about P–Ph bonds when the phenylphosphinidene ligands are in quadruply bridging but not triply bridging positions. Some related chemistry of cyclohexylphosphine is also described.

---

*Author to whom correspondence should be addressed.

0020-1693/92/$5.00

Results and discussion

Reactions of $[Ru_3(CO)_{12}]$ with phenylphosphine and cyclohexylphosphine leading to triruthenium clusters

Reaction of $[Ru_3(CO)_{12}]$ with 3 mol of PH_2R (R = Ph or Cy) per mol of Ru_3 cluster in refluxing hexane for 95 min gave a mixture of products, none in very good yield (see 'Experimental'). The previously described compounds with one P atom each, $[Ru_3H(PHPh)(CO)_{10}]$ and $[Ru_3H_2(PPh)(CO)_9]$, were obtained as a single TLC band and were not studied further. We also obtained clusters containing two P atoms, $[Ru_3H_2(PR)(CO)_8(PH_2R)]$ (R = Ph or Cy) and clusters isomeric with these, $[Ru_3H_2(PHR)_2(CO)_8]$ (R = Ph or Cy). Finally the clusters $[Ru_3H(PHR)_3(CO)_7]$ (R = Ph or Cy) containing three P atoms per cluster were obtained. The clusters $[Ru_3H_2(PHR)_2(CO)_8]$ and $[Ru_3H(PHR)_3(CO)_7]$ (R = Ph or Cy) were characterised initially by the close similarity of their IR spectra around 2000 cm^{-1} to those reported for the corresponding PPh_2 compounds [7–9]. A difference is that for each stoichiometry of the PHR complexes there is a set of isomers resulting from different stereochemistries at the asymmetric tetrahedral phosphorus atoms, however these all lead to essentially the same IR spectrum around 2000 cm^{-1}.

Much more forcing conditions, such as reaction in refluxing decane, are needed to give the dehydrogenated compound $[Ru_3(PPh)_2(CO)_9]$. This compound may also be synthesised by treating $[Ru_3H_2(PPh)(CO)_9]$ with PH_2Ph at similarly high temperatures. This reaction is expected to give initially the cluster $[Ru_3H_2(PPh)(CO)_8(PH_2Ph)]$. Indeed we have shown that $[Ru_3H_2(PCy)(CO)_8(PH_2Cy)]$ reacts with CO to give $[Ru_3(PCy)_2(CO)_9]$. Thus there is a range of triruthenium complexes containing one to three P atoms in the form of the ligands PH_2R, PHR and PR but it is difficult to get very good yields of any of these by direct reaction of $[Ru_3(CO)_{12}]$. In our work we were particularly interested in the isomers obtained when PHR ligands are incorporated into clusters and in the structures of these compounds.

Structures of the isomers $[Ru_3H_2(PPh)(CO)_8(PH_2Ph)]$ and $[Ru_3H_2(PHPh)_2(CO)_8]$

IR and ^1H NMR data are collected in Tables 1 and 2. These isomers differ in that one has a μ_3-PPh and a PH_2Ph ligand while the other has two μ_2-PHPh ligands. The structure of the former was established by NMR and a single-crystal structure determination. The hydride signal of $[Ru_3H_2(\mu_3\text{-PPh})(CO)_8(PH_2Ph)]$ appears as a 1:2:1 triplet of 1:2:1 triplets; there is coupling to the two equivalent PH_2Ph nuclei ($J = 2.0$ Hz) and virtual coupling to two ^{31}P nuclei (apparent J of the triplet = 16.2 Hz). It is a feature common to the compounds described in this paper that, since there is strong ^{31}P–^{31}P coupling, the hydride signals appear as 1:2:1 triplets or 1:3:3:1 quartets depending only upon whether there are two or three P nuclei present and this is irrespective of whether the P nuclei are equivalent or not. The PH_2Ph nuclei appear as a single ddt pattern indicating that the atoms are equivalent and that there is a symmetry plane through the Ru–PH_2Ph bond. The crystal structure (Fig. 1 and Table 3 for selected bond lengths and angles) confirms the presence of a mirror plane; atoms Ru(1), P(1), P(2), C(41), C(44), C(51) and C(54) all lie on a crystallographic mirror plane. The PH_2Ph ligand is coordinated axially *trans* to the PPh ligand with angle P(1)–Ru(1)–P(2) 159.8(1)°. The hydride ligands and the PH_2Ph atoms were located in the structure determination but were fixed in the final cycles of refinement. The compound exists both in solution and in the crystal as a single isomer.

This contrasts with the other isomer $[Ru_3H_2(PHPh)_2(CO)_8]$, which exists in three subsidiary isomeric forms in solution (see Fig. 2 for the ^1H NMR spectrum). The IR spectrum compares so closely with that of $[Ru_3H_2(PPh_2)_2(CO)_8]$ of known structure [10] that there can be no doubt about the overall skeletal

TABLE 1. IR ν(CO) data[a]

Compound	ν(CO) (cm^{-1})
$[Ru_3H(PHPh)(CO)_{10}]$	2098m, 2058s, 2048s, 2025s, 2013s, 1999m, 1989m
$[Ru_3H_2(PPh)(CO)_9]$	2103m, 2073s, 2048s, 2043m, 2029w, 2016s, 1998m, 1986w
$[Ru_3H_2(PHPh)_2(CO)_8]$	2080m, 2046s, 2035s, 2014s, 1991m, 1983w
$[Ru_3H_2(PHCy)_2(CO)_8]$	2071w, 2042s, 2035s, 2003s, 1989m, 1981w
$[Ru_3H_2(PPh)(PH_2Ph)(CO)_8]$	2075w, 2046m, 2039s, 2005s, 1998m, 1991m, 1975w
$[Ru_3H_2(PCy)(PH_2Cy)(CO)_8]$	2069w, 2034s, 2031s, 1993s, 1991m, 1979m, 1966w
$[Ru_3H(PHPh)_3(CO)_7]$	2066m, 2027s, 2023s, 2001w, 1973m
$[Ru_3H(PHCy)_3(CO)_7]$	2055m, 2014s, 1992w, 1962m
$[Ru_6H_2(PPh)_4(CO)_{12}]$	2060w, 2033s, 2025m, 2010s, 1999w, 1991w, 1968w, 1961w
$[Ru_6(PPh)_4(CO)_{12}]$	2050w, 2032s, 2027sh, 2010w, 1994w, 1988w
$[Os_6(PPh)_4(CO)_{12}]$	2057w, 2027s, 2019m, 2007s, 1998w, 1982w, 1963w, 1951w

[a]Recorded in cyclohexane solution at room temperature.

TABLE 2. ^{1}H NMR data[a]

Compound	δ	*J* (Hz)
$[Ru_3H(PHPh)(CO)_{10}]$[b]	6.70 (dd, P*H*Ph)	^1J(PH) 390.0, ^3J(HH) 3.1
	7.40 (m, Ph)	
	−16.62 (dd, Ru*H*Ru)	^2J(PH) 28.1, ^3J(HH) 3.1
$[Ru_3H_2(PHPh)_2(CO)_8]$	6.64 (dm, P*H*Ph)	^1J 362.0
	7.40 (m, Ph)	
	−17.05 (tdd, Ru*H*Ru)	^2J(PH) 24.5, ^2J(HH) 3.0, 2.5
	−16.78 (tm, Ru*H*Ru)	^2J(PH) 24.8
	−17.37 (tm, Ru*H*Ru)	^2J(PH) 22.4
	−17.58 (tdd, Ru*H*Ru)	^2J(PH) 22.1
$[Ru_3H(PHPh)_3(CO)_7]$	4.98 (dm, P*H*Ph)	^1J(PH) 361.0
	6.43 (d, br, P*H*Ph)	^1J(PH) 350.0
	8.05 (dm, P*H*Ph)	^1J(PH) 350.1
	7.30–7.66 (m, Ph)	
	−17.70 (qm, Ru*H*Ru)	^2J(PH) 18.0
$[Ru_3H_2(PPh)(PH_2Ph)(CO)_8]$	5.86 (dq, PH_2Ph)	^1J(PH) 347.6, ^3J(PH) 2.0, ^3J(HH) 2.0
	7.45 (m, C_6H_5)	
	8.00 (ddd, C_6H_5)	^3J(PH) 15.1, ^3J(HH) 9.3, ^4J(HH) 1.6
	−19.01 (tt, Ru*H*Ru)	^2J(PH) 16.2, ^3J(HH) 2.0
$[Ru_3H(PHCy)_3(CO)_7]$	4.3–7.5 (dm, P*H*Cy)	
	1.2–2.2 (m, *Cy*)	
	−18.50 (qm, Ru*H*Ru)	^2J(PH) 17.9
	−18.80 (qm, Ru*H*Ru)	^2J(PH) 17.1
	−19.20 (qm, Ru*H*Ru)	^2J(PH) 16.8
	−19.52 (qm, Ru*H*Ru)	^2J(PH) 16.7
$[Ru_3H_2(PHCy)_2(CO)_8]$	5.52 (dddd, P*H*Cy)	^1J(PH) 334.5, ^3J(HH) 7.2, ^3J(HH) 2.9
	1.3–2.1 (m, *Cy*)	
	−17.57 (tdd, Ru*H*Ru)	^2J(PH) 23.4, ^3J(HH) 3.6, ^3J(HH) 1.7
	−17.38 (tm, Ru*H*Ru)	^2J(PH) 24.2
	−17.92 (tdd, Ru*H*Ru)	^2J(PH) 22.0
	−17.78 (tm, Ru*H*Ru)	^2J(PH) 22.3
$[Ru_3H_2(PCy)(PH_2Cy)(CO)_8]$	4.56 (ddq, PH_2Cy)	^1J(PH) 337.0, ^3J(HH) 5.8, ^3J(HH) 1.9
	1.2–2.0 (m, *Cy*)	
	−19.37 (tt, Ru*H*Ru)	^2J(PH) 15.4, ^3J(HH) 3.4
$[Ru_3H(PHCy)(PH_2Cy)(CO)_9]$	5.65 (ddd, P*H*Cy)	^1J(PH) 362.0, ^3J(HH) 8.9, ^3J(HH) 2.8
	4.40 (dm, PH_2Cy)	^1J(PH) 340.0
	1.3–2.2 (m, Cy)	
	−16.82 (ddd, Ru*H*Ru)	^2J(PH) 25.2, ^3J(HH) 3.2, ^4J(HH) 1.2
$[Ru_6H_2(PPh)_4(CO)_{12}]$[b]	8.32 (br, *ortho*, 2H)	
	8.06 (ddd, *ortho*, 4H)	^3J(PH) 11.7, ^3J(HH) 6.4, ^4J(HH) 1.3
	7.48–7.60 (m, Ph, 10H)	
	7.38 (t, *meta*, 2H)	^3J(HH) 5.9
	7.34 (ddd, br, *ortho*, 2H)	^3J(PH) 13.3, ^3J(HH) 6.4
	−22.60 (br, RuH)	
$[Ru_6(PPh)_4(CO)_{12}]$[b]	8.46 (br, *ortho*, 2H)	
	7.97 (ddd, br, *ortho*, 4H)	^3J(PH) 13.7, ^3J(HH) 6.9
	7.52 (m, Ph, 6H)	
	7.58 (t, *meta*, 2H)	^3J(HH) 7.1
	7.43 (t, *para*, 2H)	^3J(HH) 7.1
	7.32 (t, *meta*, 2H)	^3J(HH) 7.6
	6.90 (br, *ortho*, 2H)	
$[Os_6PPh)_4(CO)_{12}]$[c]	8.26 (br, *ortho*, 2H)	
	7.98 (ddd, br, *ortho*, 4H)	^3J(PH) 14.1, ^3J(HH) 7.8, ^4J(HH) 1.8
	7.58 (m, Ph, 6H)	
	7.56 (t, *meta*, 2H)	^3J(HH) 7.1
	7.40 (t, *meta*, 2H)	^3J(HH) 7.1
	7.38 (t, *para*, 2H)	^3J(HH) 7.0
	6.96 (br, *ortho*, 2H)	

[a] Spectra recorded in $CDCl_3$ at 400 MHz at room temperature unless indicated otherwise. [b] Recorded at −80 °C; see Fig. 11 for changes at higher temperatures. [c] Recorded at −55 °C; spectral changes at higher temperatures very similar to those for the Ru analogue.

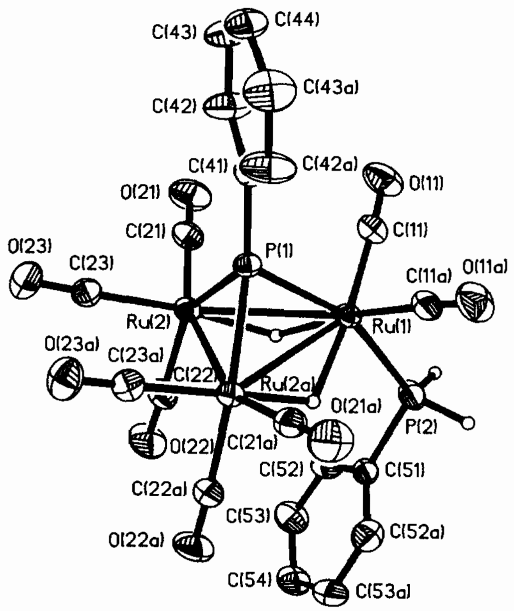

Fig. 1. Molecular structure of the cluster $[Ru_3(\mu-H)_2(\mu_3-PPh)(CO)_8(PH_2Ph)]$.

TABLE 3. Selected bond lengths (Å) and angles (°) for the cluster $[Ru_3H_2(PPh)(CO)_8(PH_2Ph)]$

Ru(1)–Ru(2)	2.948(1)	Ru(2)–C(21)	1.916(6)
Ru(2)–Ru(2a)	2.831(1)	Ru(2)–C(22)	1.955(6)
Ru(1)–P(1)	2.300(2)	Ru(2)–C(23)	1.896(6)
Ru(2)–P(1)	2.287(1)	P(1)–C(41)	1.808(7)
Ru(1)–P(2)	2.359(2)	P(2)–C(51)	1.810(8)
Ru(1)–C(11)	1.883(6)		
Ru(1)–Ru(2)–P(1)	50.2(1)	Ru(2)–Ru(1)–C(11)	96.6(2)
Ru(2)–Ru(1)–P(1)	49.8(1)	Ru(1)–Ru(2)–C(21)	101.2(2)
Ru(2a)–Ru(2)–P(1)	51.8(1)	Ru(1)–Ru(2)–C(22)	109.8(2)
Ru(1)–P(1)–Ru(2)	80.0(1)	Ru(2a)–Ru(2)–C(22)	95.1(2)
Ru(2)–P(1)–Ru(2a)	76.5(1)	Ru(2a)–Ru(2)–C(23)	94.0(2)
Ru(2)–Ru(1)–P(2)	113.6(1)		

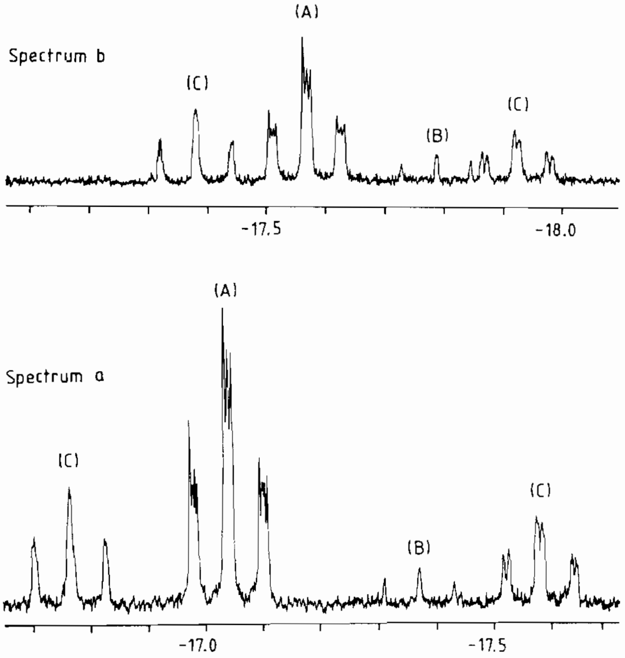

Fig. 2. ^1H NMR spectra in the hydride regions for the clusters $[Ru_3(\mu-H)_2(\mu-PHR)_2(CO)_8]$ where R = Ph (spectrum a) and R = Cy (spectrum b). The signals are labelled according to their assignments to the isomers shown in Fig. 3.

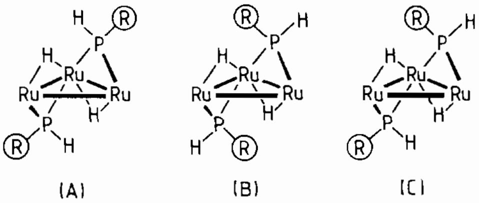

Fig. 3. Structures of the possible isomers of $[Ru_3(\mu-H)_2(\mu-PHR)_2(CO)_8]$.

geometry of the isomers. The analogous Os cluster [1, 10] as well as the Ru and Os clusters with P^tBu_2 ligands are also known [11, 12]. The three possible arrangements of the PHPh ligands as shown in Fig. 3 are therefore present in solution. Four hydride signals are observed both for the PHPh and PHCy compounds (Fig. 2). The hydrides and the P nuclei constitute an AA′XX′ spectrum with additional fine structure from ^1H–^1H coupling. The isomers (A) and (B) in Fig. 3 have C_2 symmetry and would each give a single hydride resonance whereas isomer (C) has non-equivalent hydride ligands and would give two hydride triplets. Assuming that the R groups are more favourably positioned pointing outwards, the labels on the signals in Fig. 2 correspond with the isomers in Fig. 3, although we cannot make assignments without making this assumption. We have not been able to separate the isomers by TLC but it is unlikely that these are interconverting. No changes in the ^1H NMR spectra were observed with change of temperature nor with prolonged irradiation with white light.

Structures of $[Ru_3(\mu-H)(PHR)_3(CO)_7]$ (R = Ph or Cy)

The PHPh compound was isolated as a deep orange air-stable crystalline solid by TLC. The hydride resonance appeared as a quartet at δ −17.70 and there are three equal intensity P*H* signals. A stoichiometry with three PHR ligands was confirmed by its mass spectrum and analytical data. As with $[Ru_3(\mu-H)_2(\mu-PHPh)_2(CO)_8]$ there are several possible isomers for this compound and it is surprising that only one was isolated by TLC and crystallisation. It is unlikely that only one isomer was formed in view of the results for the PHCy compound (see below), but there must have been a fortuitous isolation of one rather than any other isomers. The structure was presumed to be based on those established earlier for $[Ru_3(\mu-H)(\mu-PPh_2)_3(CO)_7]$

[9] and $[Os_3(\mu\text{-}H)(\mu\text{-}PCy_2)_3(CO)_7]$ [11] but we determined the crystal structure nonetheless to establish the stereochemistries at the phosphorus atoms. There are potentially six isomers having the overall geometry with a PHR group along each Ru–Ru edge of the triangle, two above and one below the Ru_3 plane (see Fig. 4). The observed structure of the compound which we crystallised is shown in Fig. 5 and selected bond lengths and angles are in Table 4. The molecular structure corresponds with structure (C) in Fig. 4 (although the opposite enantiomers are illustrated). This accounts for there being three different P*H*Ph NMR signals. Based on the positions of the CO ligands the hydride bridges the Ru(1)–Ru(2) edge *trans* to the ligands C(11)O(11) and C(22)O(22) and as found for the related structure with PPh_2 ligands [9].

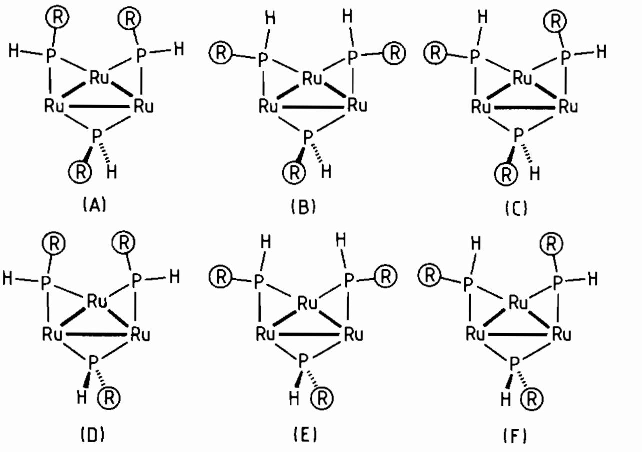

Fig. 4. Structures of the possible isomers of $[Ru_3(\mu\text{-}H)(\mu\text{-}PHR)_3(CO)_7]$.

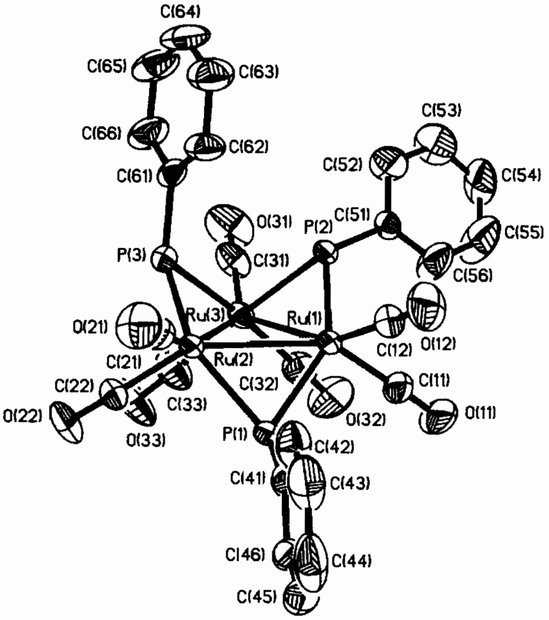

Fig. 5. Molecular structure of the cluster $[Ru_3(\mu\text{-}H)(\mu\text{-}PHPh)_3(CO)_7]$.

TABLE 4. Selected bond lengths (Å) and angles (°) for the cluster $[Ru_3H(PHPh)_3(CO)_7]$

Ru(1)–Ru(2)	2.801(1)	P(2)–C(51)	1.816(8)
Ru(2)–Ru(3)	2.965(1)	P(3)–C(61)	1.800(9)
Ru(1)–Ru(3)	2.956(1)	Ru(1)–C(11)	1.880(9)
Ru(1)–P(1)	2.327(2)	Ru(1)–C(12)	1.876(9)
Ru(2)–P(1)	2.320(2)	Ru(2)–C(21)	1.856(9)
Ru(1)–P(2)	2.304(2)	Ru(2)–C(22)	1.88(1)
Ru(3)–P(2)	2.386(2)	Ru(3)–C(31)	1.90(1)
Ru(2)–P(3)	2.309(2)	Ru(3)–C(32)	1.93(1)
Ru(3)–P(3)	2.387(2)	Ru(3)–C(33)	1.91(1)
P(1)–C(41)	1.812(9)		
Ru(1)–P(1)–Ru(2)	74.1(1)	Ru(2)–Ru(3)–P(2)	89.9(1)
Ru(1)–P(2)–Ru(3)	78.1(1)	Ru(2)–Ru(3)–P(3)	49.7(1)
Ru(2)–P(3)–Ru(3)	78.3(1)	Ru(3)–Ru(2)–P(1)	92.5(1)
Ru(1)–Ru(2)–P(1)	53.1(1)	Ru(3)–Ru(2)–P(3)	52.0(1)
Ru(1)–Ru(2)–P(3)	98.1(1)	Ru(1)–P(1)–C(41)	121.3(3)
Ru(2)–Ru(1)–P(1)	52.8(1)	Ru(2)–P(1)–C(41)	122.9(3)
Ru(2)–Ru(1)–P(2)	95.8(1)	Ru(1)–P(2)–C(51)	127.2(3)
Ru(1)–Ru(3)–P(2)	49.7(1)	Ru(3)–P(2)–C(51)	120.9(3)
Ru(1)–Ru(3)–P(3)	92.2(1)	Ru(2)–P(3)–C(61)	129.9(3)
Ru(3)–Ru(1)–P(1)	92.5(1)	Ru(3)–P(3)–C(61)	120.5(3)
Ru(3)–Ru(1)–P(2)	52.2(1)		

Also as in the earlier structures, the phosphido bridges that lie above the Ru_3 plane are unsymmetrical. The Ru–P bond lengths to the $Ru(CO)_3$ unit (Ru(3)–P(2), 2.386(2); Ru(3)–P(3), 2.387(2) Å) are significantly longer than the lengths of these P atoms to the $Ru(CO)_2$ units (Ru(1)–P(2), 2.304(2); Ru(2)–P(3), 2.309(2) Å). The Ru–P distances to the remaining PHPh ligand below the Ru_3 plane are of intermediate value (Ru(1)–P(1), 2.327(2); Ru(2)–P(1), 2.320(2) Å). The longer distances to the $Ru(CO)_3$ unit probably have an electronic origin and this feature is found in the other related structures with different phosphido bridges that have been determined.

The corresponding compound $[Ru_3H(PHCy)_3(CO)_7]$ was also obtained as deep orange microcrystals after TLC and gives a pattern for the ν(CO) absorptions similar to that of the PHPh compound except that the wavenumbers are lower because of the better donor properties of PHCy compared with PHPh bridges (see Table 1). This is very good evidence for an entirely analogous structure but curiously the PHCy complex shows four instead of one ^1H NMR hydride resonances (δ −18.50, −18.80, −19.20 and −19.52) all of which are virtual 1:3:3:1 quartets like that for the PHPh compound (see Fig. 6). Clearly there are isomers present in this case. The P*H* region of the spectrum is very complex and at least eight signals (all doublets with *J*(PH) 350–370 Hz) being apparent. We interpret this in terms of four of the isomers in Fig. 4 being present. Possibly isomers (A) and (D) with adjacent Cy groups

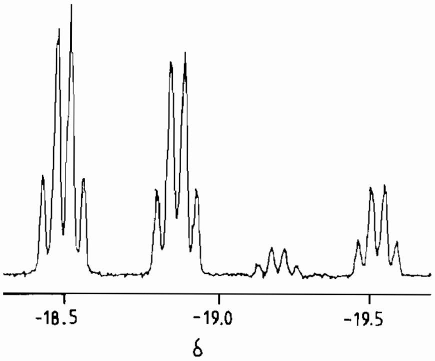

Fig. 6. ^1H NMR spectrum of the cluster $[Ru_3(\mu\text{-}H)(\mu\text{-}PHCy)_3(CO)_7]$ in the hydride region showing that there are four isomeric forms in solution.

are less favourable so that isomers (B), (C), (E) and (F) are those most likely to be present in solution. For these isomers we would predict a total of ten P*H* doublets so there would need to be some accidental overlap of signals to account for the observed eight signals. No exchange of the isomers on the NMR time scale up to 55 °C was observed and visible photolysis did not alter the abundances. Attempts to separate the isomers were unsuccessful.

Other compounds related to the PH_2Ph-derived species are formed from PH_2Cy and are given in 'Experimental' and the Tables.

Thermolysis and hydrogenation of $[Ru_3(PPh)_2(CO)_9]$

We isolated this known compound from the reaction of $[Ru_3(CO)_{12}]$ with PH_2Ph in refluxing decane, the yield at best being only 15%. This cluster is probably formed by dehydrogenation and carbonylation of the isomeric clusters $[Ru_3H_2(PPh)(CO)_8(PH_2Ph)]$ and/or $[Ru_3H_2(PHPh)_2(CO)_8]$. We showed that the thermolysis of $[Ru_3H_2(PCy)(CO)_8(PH_2Cy)]$ in refluxing n-decane with a purge of CO leads to $[Ru_3(PCy)_2(CO)_9]$. The bis-phosphinidene complexes are very stable/unreactive. We attempted to hydrogenate $[Ru_3(PPh)_2(CO)_9]$ at high temperatures back to the above isomers with higher hydrogen contents but failed since only Ru_6 condensation products were obtained. Once formed the PPh ligand is very robust and generally is carried through reactions. Thermolysis of $[Ru_3(PPh)_2(CO)_9]$ in refluxing decane with a purge of H_2 until little starting material remained gave a deep brown material which was separated by TLC to give three products: the known compound $[Ru_6(PPh)_4(CO)_{12}]$, the new cluster $[Ru_6H_2(PPh)_4(CO)_{12}]$ which is a hydrogen adduct of the first, and a third unknown higher cluster which we were unable to characterise because it was in such low yield. Similar treatment using N_2 instead of H_2 as the purging gas also gave the three same products so the hydride ligand is not necessarily formed from H_2. However, we were able to show that hydrogen adds to $[Ru_6(PPh)_4(CO)_{12}]$ to give the dihydride. Using CO instead of either of these gases suppressed the reaction totally and starting $[Ru_3(PPh)_2(CO)_9]$ was recovered.

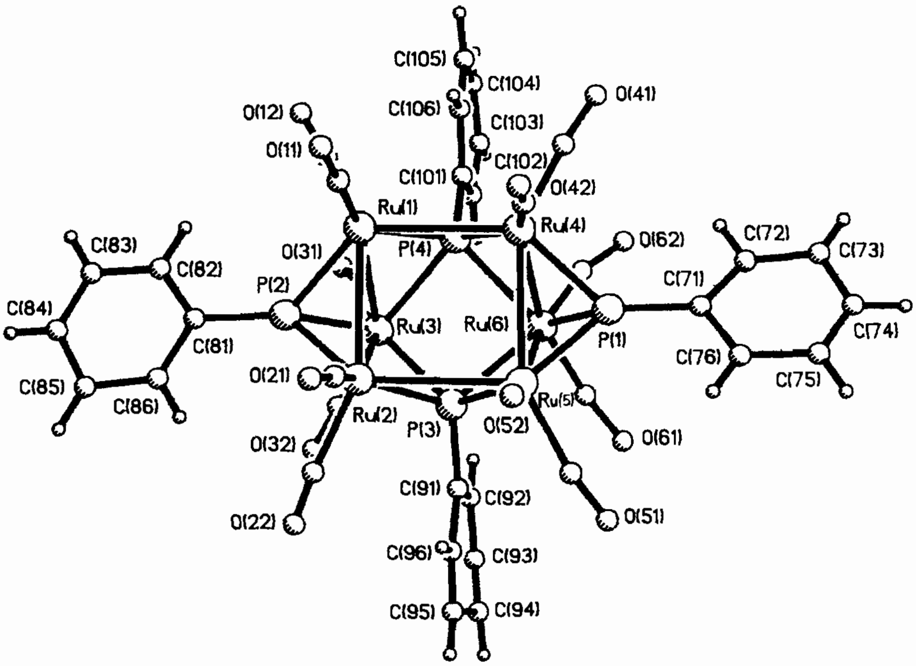

Fig. 7. Molecular structure of the cluster $[Ru_6H_2(\mu_3\text{-}PPh)_2(\mu_4\text{-}PPh)_2(CO)_{12}]$; the hydride ligands are not shown as their positions are uncertain.

The Ru_6 compounds do not easily breakdown to $[Ru_3(PPh)_2(CO)_9]$ with CO so we believe that there is a preliminary reversible CO dissociation step in the condensation reaction.

The nature of the decarbonylation and dimerisation of $[Ru_3(PPh)_2(CO)_9]$ remains unclear but probably after decarbonylation there is dimerisation with one of the μ_3-ligands at each Ru_3 unit then opening up to μ_2 at that unit and bridging to the other Ru_3 group. These PPh ligands eventually occupy μ_4 sites.

The known compound $[Ru_6(PPh)_4(CO)_{12}]$ has been structurally characterised twice in different crystalline forms, one with and one without a benzene of crystallisation. The two molecular geometries are very similar and based on a highly distorted trigonal prismatic Ru_6 cage with both triangular faces capped by μ_3-PPh and two of the three rectangular faces capped by μ_4-PPh. The nature of the distortion has been discussed but the effect of it is to allow further Ru–Ru contacts across the diagonals of the distorted 'rectangular' faces. The cluster has an 88 valence electron count (88 VEC) and the dihydride we isolated has a 90 VEC so the structural consequence of changing the VEC by the addition of two electrons could be studied. Apart from the Ph resonances which are very similar for the two compounds (see later), the dihydride contained a broad ^1H NMR resonance at δ −22.60 which showed no fine structure at 35 °C nor on cooling to −80 °C. We believed on this spectral evidence that the overall structures, that is with two μ_3- and two μ_4-PPh ligands, are the same for the two compounds.

TABLE 5. Selected bond lengths (Å) and angles (°) for the cluster $[Ru_6H_2(PPh)_4(CO)_{12}]$

Ru(1)–Ru(2)	2.976(4)	Ru(1)–Ru(3)	2.835(4)
Ru(1)–Ru(4)	3.068(3)	Ru(2)–Ru(3)	2.825(4)
Ru(2)–Ru(5)	3.080(4)	Ru(3)...Ru(6)	3.277(4)
Ru(4)–Ru(5)	2.953(4)	Ru(4)–Ru(6)	2.877(4)
Ru(5)–Ru(6)	2.852(4)	Ru(1)–P(2)	2.278(8)
Ru(2)–P(2)	2.236(8)	Ru(3)–P(2)	2.279(10)
Ru(4)–P(1)	2.266(9)	Ru(5)–P(1)	2.259(8)
Ru(6)–P(1)	2.306(9)	Ru(2)–P(3)	2.338(10)
Ru(3)–P(3)	2.390(8)	Ru(5)–P(3)	2.319(8)
Ru(6)–P(3)	2.467(9)	Ru(1)–P(4)	2.311(9)
Ru(3)–P(4)	2.472(7)	Ru(4)–P(4)	2.376(8)
Ru(6)–P(4)	2.442(8)		
Range of Ru–P for μ_3-PPh = 2.236–2.306 (av. 2.271)			
Range of Ru–P for μ_4-PPh = 2.311–2.467 (av. 2.389)			
Ru(1)–Ru(2)–Ru(3)	58.4(1)	Ru(1)–Ru(3)–Ru(2)	63.4(1)
Ru(2)–Ru(1)–Ru(3)	58.1(1)	Ru(4)–Ru(5)–Ru(6)	59.4(1)
Ru(4)–Ru(6)–Ru(5)	62.1(1)	Ru(5)–Ru(4)–Ru(6)	58.6(1)
Ru(3)–Ru(1)–Ru(4)	92.2(1)	Ru(2)–Ru(1)–Ru(4)	87.0(1)
Ru(3)–Ru(2)–Ru(5)	91.8(1)	Ru(1)–Ru(2)–Ru(5)	92.5(1)
Ru(6)–Ru(4)–Ru(1)	91.8(1)	Ru(5)–Ru(4)–Ru(1)	93.2(1)
Ru(6)–Ru(5)–Ru(2)	92.1(1)	Ru(4)–Ru(5)–Ru(2)	87.1(1)
Ru(4)–P(1)–Ru(5)	81.5(3)	Ru(4)–P(1)–Ru(6)	78.0(3)
Ru(5)–P(1)–Ru(6)	77.3(2)	Ru(1)–P(2)–Ru(2)	82.5(2)
Ru(1)–P(2)–Ru(3)	76.9(3)	Ru(2)–P(2)–Ru(3)	77.5(3)
Ru(2)–P(3)–Ru(3)	73.4(3)	Ru(2)–P(3)–Ru(5)	82.8(3)
Ru(3)–P(3)–Ru(6)	84.8(3)	Ru(5)–P(3)–Ru(6)	73.1(2)
Ru(1)–P(4)–Ru(3)	72.6(2)	Ru(1)–P(4)–Ru(4)	81.7(3)
Ru(3)–P(4)–Ru(6)	83.6(2)	Ru(4)–P(4)–Ru(6)	73.3(2)

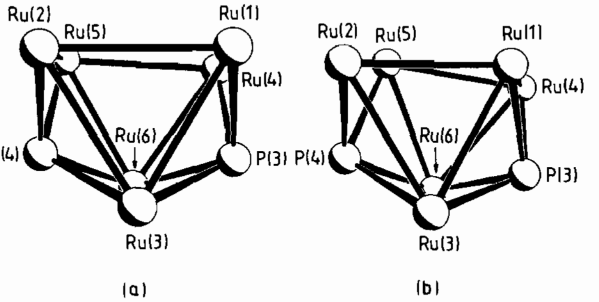

Fig. 8. Structures of the $Ru_6(\mu_4\text{-}P)_2$ sets of atoms for the clusters (a) $[Ru_6H_2(\mu_3\text{-}PPh)_2(\mu_4\text{-}PPh)_2(CO)_{12}]$ and (b) the non-hydrido analogue of this, viewed approximately perpendicularly to the triangular Ru_3 faces.

The molecular structure of $[Ru_6H_2(PPh)_4(CO)_{12}]$ is displayed in Fig. 7 and selected bond lengths and angles are in Table 5. The overall arrangement with six Ru atoms and bridging PPh ligands, two μ_3 and two μ_4, was as expected but the distortions from a regular trigonal prismatic geometry are much less than for the non-hydride. The quality of the structure was not good because of the difficulty in growing very good crystals; the e.s.d. values are quite high and the hydride ligands could not be located. Even a careful analysis of the positions of the other ligands does not allow us to suggest hydride positions and this is still an open question. It is only the ^1H NMR spectrum and the very different structure from that of the non-hydride that allowed us to establish their presence. Figure 8 shows projections approximately perpendicular to the Ru_3 triangular faces for the two compounds illustrating the more regular shape of the dihydride and how the 'rectangular' faces of the trigonal prism are much more closely rectangular. This is reinforced by the narrow range of the diagonal distances of the rectangular faces of the dihydride: Ru(3)–Ru(5) 4.265(4), Ru(2)–Ru(6) 4.244(4), Ru(1)–Ru(6) 4.257(4), Ru(3)–Ru(4) 4.267(4), Ru(1)–Ru(5) 4.161(4) and Ru(2)–Ru(4) 4.374(4) Å, none of which is short enough to imply any kind of even weak bonding interaction. The corresponding six distances for the diagonals of $[Ru_6(PPh)_4(CO)_{12}]$ are 4.319, 3.920, 4.346, 3.939, 4.663 and 3.212 Å. This wide variation is probably the result of the need for a fairly short Ru–Ru distance (3.212 Å) for one of the diagonals.

Likewise Ru–Ru distances between the two triangular faces are not very different from each other in the dihydride (Ru(1)–Ru(4), 3.068(3), Ru(2)–Ru(5), 3.080(4), Ru(3)–Ru(6), 3.268(4) Å). The last of these distance is normally considered too long for a bond and is not shown as one in Fig. 7. The corresponding

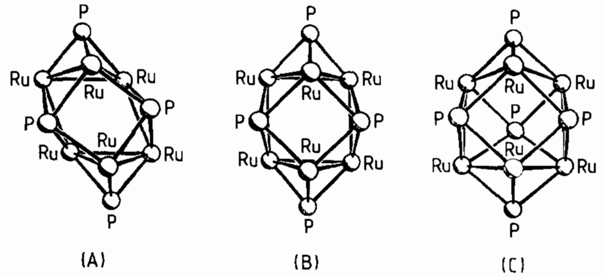

Fig. 9. A comparison of the arrangements of the Ru and P atoms in the clusters $[Ru_6(PPh)_4(CO)_{12}]$ (88 VEC) (A), $[Ru_6H_2(PPh)_4(CO)_{12}]$ (90 VEC) (B) and $[Ru_6(PPh)_5(CO)_{12}]$ (92 VEC) (C).

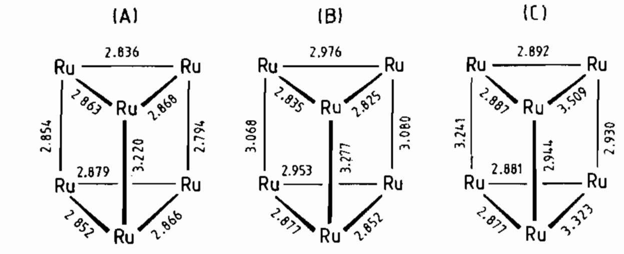

VEC	88	90	92
Average intrabasal distance/Å	2.861	2.886	3.062
Average interbasal distance/Å	2.956	3.139	3.038
Average of all 9 Ru-Ru distances/Å	2.892	2.970	3.054

Fig. 10. Ru–Ru bond lengths in the clusters $[Ru_6(PPh)_4(CO)_{12}]$ (88 VEC) (A), $[Ru_6H_2(PPh)_4(CO)_{12}]$ (90 VEC) (B) and $[Ru_6(PPh)_5(CO)_{12}]$ (92 VEC) (C) with some averaged distances.

distances in $[Ru_6(PPh)_4(CO)_{12}]$ are 2.854(1), 2.794(1) and 3.220(2) Å. Figure 9 shows the shapes and Fig. 10 summarises Ru–Ru distances in three related Ru_6 compounds with 88, 90 and 92 VEC, respectively. Clearly a reduction in the VEC leads to a shortening of the Ru–Ru distances within the triangular faces. The averages of the nine Ru–Ru distances (six in the triangular faces and three between these faces) in the 88, 90 and 92 VEC clusters are 2.892, 2.970 and 3.054 Å, respectively, which indicated a fairly steady expansion with increasing VEC. There is a steady Ru–Ru expansion in the triangular faces but not in the interfacial distances. This is a consequence of the three μ_4-PPh ligands in $[Ru_6(PPh)_5(CO)_{12}]$ not allowing the triangular faces to separate so easily. Certainly the overall picture is the occupancy of Ru–Ru antibonding orbitals by the additional valence electrons.

Fluxionality of the hexanuclear clusters

An interesting feature of the ^1H NMR spectra of $[Ru_6(PPh)_4(CO)_{12}]$ and the dihydride derivative $[Ru_6H_2(PPh)_4(CO)_{12}]$ is that the phenyl resonances of both compounds, especially the *ortho* resonances, are similarly strongly temperature dependent. Figure 11 shows the changes in the NMR spectra for the two compounds. In essence the resonances for two PPh groups in each compound are temperature independent whereas the other two PPh groups in each compound show non-equivalent *ortho* resonces (marked a) at −75 °C which coalesce to single resonances at around room temperature (marked b), with coalescence temperature around 0 °C in each case. These effects result from restricted rotation about the P–Ph bonds in either the μ_3- or the μ_4-ligands and based on the crystal structures we can confidently identify the μ_4-ligands as the ones with the high rotational barriers. As shown in Fig. 7 the μ_4-PPh rings lie approximately parallel to the triangular Ru_3 faces so that the *ortho* sites are very

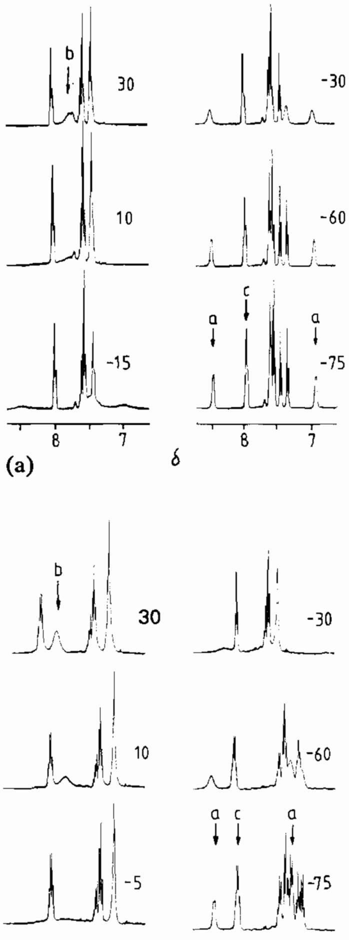

Fig. 11. ^1H NMR spectra in the phenyl region for (a) the non-hydrido cluster $[Ru_6(PPh)_4(CO)_{12}]$ and (b) the dihydrido cluster $[Ru_6H_2(PPh)_4(CO)_{12}]$. Peaks marked a for the *ortho* hydrogen atoms of the μ_4-PPh ligands coalesce to peaks marked b, while those marked c are for the *ortho* hydrogen atoms of the μ_3-PPh ligands. Temperatures (°C) are given by each spectrum.

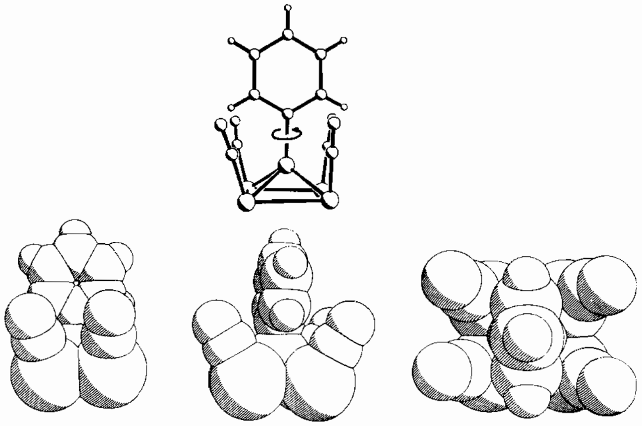

Fig. 12. Three space filling views of one of the $Ru_4(CO)_4(\mu_4$-PPh) units of the cluster $[Ru_6H_2(\mu_3\text{-PPh})_2(\mu_4\text{-PPh})_2(CO)_{12}]$ taken from crystallographic data to show the steric origin of the restricted rotation about the P–Ph bonds.

different; the chemical shift difference is 1 ppm or greater. The *ortho* sites of the μ_3-PPh ligands are very closely similar so that restricted rotation would not be expected to be apparent for these anyway. Figure 12 shows very clearly how the μ_4-ligands slot in between four CO ligands pointing out from the rectangular Ru_4 face. Simple space-filling drawings show that there will be quite severe clashes between these CO ligands and the *ortho* hydrogen atoms on rotation and accounts simply for the restricted rotation.

Experimental

The compounds $[Ru_3(CO)_{12}]$, phenylphosphine and cyclohexylphosphine were used as supplied to us by Aldrich plc. Reactions were all carried out under nitrogen but room temperature work-up was in air; all the isolated products are stable in air at room temperature. The light petroleum used as eluant for TLC on SiO_2 had the boiling temperature range 30–40 °C.

Reaction of $[Ru_3(CO)_{12}]$ with phenylphosphine

The colour of a solution of $[Ru_3(CO)_{12}]$ (0.404 g, 0.63 mmol) and phenylphosphine (0.278 cm^3, 2.5 mmol) in n-hexane (80 cm^3) under reflux for 95 min changed from deep orange to pale yellow. The solvent was removed under reduced pressure to give a deep yellow oil. Chromatography (TLC: eluant, light petroleum/dichloromethane (9:1 vol./vol.)) gave three well-separated bands. The fastest was a mixture of the two known compounds: $[Ru_3(\mu\text{-H})(\mu\text{-PHPh})(CO)_{10}]$ and $[Ru_3(\mu\text{-H})_2(\mu_3\text{-PPh})(CO)_9]$ (0.106 g, 25% yield total). Further heating of this mixture in refluxing heptane gave the pure nonacarbonyl. The next band eluted was extracted with dichloromethane, the solvent was removed, and the yellow oil treated with n-hexane to give red crystals (0.013 g, 3%) of $[Ru_3(\mu\text{-H})_2(\mu\text{-PHPh})_2(CO)_8]$, characterised initially by the similarity of its IR spectrum with that of $[Ru_3(\mu\text{-H})_2(\mu\text{-PPh}_2)(CO)_8]$ [7–10]. Its NMR spectra showed the presence of three isomers which could not be separated. The slowest moving band showed the presence of a mixture of two compounds. Crystallisation from n-hexane gave deep orange crystals of the cluster $[Ru_3(\mu\text{-H})(\mu\text{-PHPh})_3(CO)_7]$ (0.009 g, 3%) characterised by the similarity of its IR spectra with that of $[Ru_3(\mu\text{-H})(\mu\text{-PPh}_2)_3(CO)_7]$ [9] and by single-crystal structure determination (see below). MS(EI): *m/e* (parent molecular ion) = 826 based on ^{101}Ru; fragmentation pattern: $826-28x$ where $x=1$–7. Crystallisation of the hexane mother liquor gave a mixture of orange crystals of $[Ru_3(\mu\text{-H})(\mu\text{-PHPh})_3(CO)_7]$ and yellow crystals which were selected (0.007 g, 1.5%) and characterised spectroscopically and by X-ray structure determination as $[Ru_3(\mu\text{-H})(\mu_3\text{-PPh})(PH_2Ph)(CO)_8]$.

Reaction of $[Ru_3(CO)_{12}]$ with cyclohexylphosphine

A deep orange solution of $[Ru_3(CO)_{12}]$ (0.174 g, 0.27 mmol) and cyclohexylphosphine (0.11 g, 1.0 mmol) in n-hexane (100 cm^3) heated under reflux for 95 min became pale yellow. Removal of the solvent and TLC (eluant: light petroleum/dichloromethane (18:1 vol./vol.)) gave three major bands. The fastest gave red crystals (0.0098 g) from n-hexane at −20 °C characterised as the cluster $[Ru_3(\mu\text{-H})_2(\mu\text{-PHCy})_2(CO)_8]$. *Anal.* Found: C, 31.35; H, 3.2. Calc. for $C_{20}H_{26}O_8P_2Ru_3$: C, 31.6; H, 3.4%. MS(EI): *m/e* (parent molecular ion) = 757 based on ^{101}Ru, fragmentation pattern $757-28x$ where $x=1$–8. The next band gave deep orange crystals (0.007 g) from n-hexane (−20 °C) characterised as the cluster $[Ru_3(\mu\text{-H})(\mu\text{-PHCy})_3(CO)_7]$. *Anal.* Found: C, 35.05; H, 4.4. Calc. for $C_{25}H_{37}O_7P_3Ru_3$: C, 35.8; H, 4.4%. MS(EI): *m/e* (parent molecular ion) = 846 based on ^{101}Ru, fragmentation pattern: $846-28x$ where $x=1$–7. The slowest band gave deep red crystals (0.014 g) of the cluster $[Ru_3(\mu\text{-H})(\mu_3\text{-PHCy})(PH_2Cy)(CO)_9]$ from n-hexane over several days at −20 °C. *Anal.* Found: C, 31.7; H, 3.35. Calc. for $C_{21}H_{26}O_9P_3Ru_3$: C, 32.0; H, 3.3%. Over a further period at -20 °C red–orange crystals (0.008 g) were deposited and characterised as $[Ru_3(\mu\text{-H})_2(\mu_3\text{-PCy})(PH_2Cy)(CO)_8]$. *Anal.* Found: C, 31.55; H, 3.5. Calc. for $C_{20}H_{26}O_8P_2Ru_3$: C, 31.6; H, 3.4%. MS(EI): *m/e* (parent molecular ion) = 857 based on ^{101}Ru, fragmentation pattern: $857-28x$ where $x=1$–8.

Preparation of $[Ru_3(\mu_3\text{-PPh})_2(CO)_9]$

A refluxing solution of $[Ru_3(CO)_{12}]$ (0.269 g, 0.40 mmol) and phenylphosphine (0.15 cm^3, 1.4 mmol) in n-decane (60 cm^3) changed from deep orange to brown over 70 min. The solvent was removed under reduced pressure and the residue pumped at *c.* 0.1 mm Hg. TLC (eluant: light petroleum/dichloromethane (6:1 vol./vol.)) gave one fast moving yellow band of the product (0.047 g, 15%), characterised by comparison of its spectra with those reported [5, 6].

Reaction of [$Ru_3(\mu$-$H)_2(\mu_3$-$PPh)(CO)_9$] with phenylphosphine

Carbon monoxide was bubbled through a refluxing solution of the cluster (0.023 g, 0.035 mmol) and phenylphosphine (0.007 g, 0.035 mmol) in n-decane (20 cm^3) for 90 min. The IR spectrum after this time showed that [$Ru_3(\mu_3$-$PPh)_2(CO)_9$] was present and the spectrum was showing little change with time. TLC of the deep brown residue after removal of the solvent (eluant: light petroleum/dichloromethane (6:1 vol./vol.)) gave a single product characterised as [$Ru_3(\mu_3$-$PPh)_2(CO)_9$] (0.0132 g, 48%).

Treatment of [$Ru_3(\mu$-$H)_2(\mu_3$-$PCy)(PH_2Cy)(CO)_8$] with carbon monoxide

CO was bubbled through a refluxing solution of the cluster (0.003 g) in n-decane (10 cm^3) for 300 min until there was no further change in the IR spectrum. TLC work-up after removal of the solvent under reduced pressure (eluant: light petroleum/dichloromethane (3:1 vol./vol.)) gave just one major yellow band giving the known compound [$Ru_3(\mu_3$-$PCy)_2(CO)_9$] (0.0006 g) which was characterised spectroscopically.

Attempted hydrogenation of [$Ru_3(\mu_3$-$PPh)_2(CO)_9$]

When hydrogen was purged through a refluxing solution of the cluster (0.0132 g) in n-decane (20 cm^3) for 150 min, the IR spectrum showed that little starting material remained. The deep brown residue after removal of the solvent was separated by TLC (eluant: light petroleum/dichloromethane (3:1 vol./vol.)) to give three well-separated bands. Deep orange–red crystals (0.003 g) obtained from the top band by slow evaporation of a n-hexane solution were characterised as [$Ru_6(\mu$-$H)_2(\mu_3$-$PPh)_2(\mu_4$-$PPh)_2(CO)_{12}$]. *Anal.* Found: C, 30.75; H, 1.65. Calc. for $C_{36}H_{22}O_{12}P_4Ru_6$: C, 31.4; H, 1.6%. MS(FAB): *m/e* (parent molecular ion) = 1374 based on ^{101}Ru, fragmentation pattern: 1374 − 28*x* where *x* = 1–12. The second TLC band gave deep brown crystals (0.005 g) by slow evaporation of a n-hexane solution at room temperature which were characterised as the known compound [$Ru_6(\mu_3$-$PPh)_2(\mu_4$-$PPh)_2(CO)_{12}$]. *Anal.*

TABLE 6. Crystal data and details of data collection, structure solution and refinement for the compounds [$Ru_3H_2(PPh)(PH_2Ph)(CO)_8$], [$Ru_3H(PHPh)_3(CO)_7$] and [$Ru_6H_2(PPh)_4(CO)_{12}$][a]

Formula	$C_{20}H_{14}O_8P_2Ru_3$	$C_{25}H_{19}O_7P_3Ru_3$	$C_{36}H_{22}O_{12}P_4Ru_6$
M (g mol^{-1})	747.49	827.56	1367.88
Colour	yellow	deep orange	deep red
Size (mm)	0.20×0.15×0.20	0.10×0.15×0.30	0.30×0.20×0.08
Crystal system	monoclinic	monoclinic	triclinic
Space group	$P2_1/m$	$P2_1/n$	$P\bar{1}$
a (Å)	9.493(2)	8.433(2)	10.144(3)
b (Å)	12.557(3)	24.852(5)	12.452(4)
c (Å)	10.614(2)	14.641(6)	18.204(6)
α (°)	90	90	88.02(3)
β (°)	94.98(2)	95.91(3)	77.80(2)
γ (°)	90	90	72.72(2)
U (Å^3)	1260.5(5)	3052(1)	2145(1)
Z	2	4	2
D_c (g cm^{-3})	1.97	1.80	2.13
μ(Mo Kα) (cm^{-1})	19.1	16.3	22.2
F(000)	720	1608	1316
No. orientation reflections; 2θ range (°)	45; 9–30	28; 12–26	33; 8–26
Total data	2442	5925	8460
Unique data	2299	5387	7362
Reject criterion	$I_o \leqslant 1.5\sigma(I_o)$	$I_o \leqslant 1.5\sigma(I_o)$	$I_o \leqslant 5\sigma(I_o)$
Reflections used in refinement	1983	4302	3713
Parameters	161	343	238
R^b	0.0345	0.0539	0.0986
R_w^c	0.0423	0.0465	0.1082
g^d	0.00282	0.00023	0.000064
Max. shift/e.s.d. in final L.S.	0.001	0.001	0.007
Max. peak in final difference Fourier (e Å^{-3})	0.44	0.93	1.73

[a] Common to each determination: Nicolet R3v/m diffractometer; data collected at 23 °C with Mo Kα radiation (λ = 0.71073 Å) with scan mode ω–2θ in the range $5 \leqslant 2\theta \leqslant 50$°; direct methods solution. [b] $R = \Sigma(|F_o| - |F_c|)/\Sigma|F_o|$. [c] $R_w = [\Sigma w(|F_o| - |F_c|)^2/\Sigma w|F_o|^2]^{1/2}$. [d] $w = 1/[\sigma^2(F_o) + gF_o^2]$.

Found: C, 31.45; H, 1.4. Calc. for $C_{36}H_{20}O_{12}P_4Ru_6$: C, 31.45; H, 1.45%. The slowest band gave a very small amount of dark brown crystals which could not be characterised. A similar treatment of $[Ru_3(\mu_3\text{-}PPh)_2(CO)_9]$ to the above but using nitrogen instead of hydrogen for the purge gave the same three compounds in similar yield; in this case we have not accounted for the hydrido ligands. Using CO instead of N_2 or H_2 for the purge gave no reaction over several hours; TLC gave an essentially quantitative recovery of starting material.

Hydrogenation of $[Ru_6(\mu_3\text{-}PPh)_2(\mu_4\text{-}PPh)_2(CO)_{12}]$

A refluxing solution of the compound (0.0112 g) in mesitylene (20 cm^3) was purged with hydrogen gas for 45 min by which time the IR spectrum showed that much of the starting material had been converted. TLC work-up as above gave the starting hexaruthenium cluster (0.0025 g, 22%) and $[Ru_6(\mu\text{-}H)_2(\mu_3\text{-}PPh)_2(\mu_4\text{-}PPh)_2(CO)_{12}]$ (0.0064 g, 57%).

Thermolysis of $[Os_3(\mu_3\text{-}PPh)_2(CO)_9]$

Treatment of this compound (0.0122 g) in refluxing tetrahydronaphthalene (10 cm^3) for 180 min followed by TLC on silica as above gave a single major brown band. Extraction into dichloromethane, removal of this solvent and recrystallisation by slow evaporation of a hexane solution gave deep brown crystals of $[Os_6(PPh)_4(CO)_{12}]$ (0.003 g). *Anal.* Found: C, 19.25; H, 0.7. Calc. for $C_{36}H_{20}O_{12}Os_6P_4$: C, 20.0, H, 1.05%.

TABLE 7. Fractional atomic coordinates ($\times 10^4$) for the cluster $[Ru_3H_2(PPh)(CO)_8(PH_2Ph)]$

	x	y	z
Ru(1)	4568(1)	2500	6066(1)
Ru(2)	3073(1)	3627(1)	7989(1)
P(1)	4970(2)	2500	8234(2)
P(2)	3331(2)	2500	4040(2)
C(41)	6673(7)	2500	9139(7)
C(42)	7335(7)	3436(6)	9486(9)
C(43)	8634(9)	3431(7)	10165(9)
C(44)	9237(10)	2500	10525(10)
C(51)	1417(8)	2500	3920(7)
C(52)	694(7)	3441(6)	3900(7)
C(53)	−757(7)	3454(6)	3864(8)
C(54)	−1469(10)	2500	3836(9)
C(11)	5836(6)	3606(5)	5767(6)
O(11)	6554(5)	4310(4)	5622(6)
C(21)	3788(6)	5045(5)	7842(6)
O(21)	4215(6)	5868(4)	7728(6)
C(22)	1070(6)	3765(5)	7411(6)
O(22)	−101(5)	3834(5)	7107(5)
C(23)	2784(7)	3733(4)	9729(6)
O(23)	2639(6)	3798(4)	10767(4)

TABLE 8. Fractional atomic coordinates ($\times 10^4$) for the cluster $[Ru_3H(PHPh)_3(CO)_7]$

	x	y	z
Ru(1)	2936(1)	994(1)	5786(1)
Ru(2)	1059(1)	1767(1)	6560(1)
Ru(3)	539(1)	1582(1)	4551(1)
P(1)	1152(3)	851(1)	6873(1)
P(2)	3345(2)	1490(1)	4502(1)
P(3)	988(2)	2398(1)	5399(1)
C(41)	1810(12)	582(4)	7999(6)
C(42)	3129(14)	778(5)	8508(7)
C(43)	3596(16)	588(6)	9370(8)
C(44)	2783(23)	184(7)	9737(9)
C(45)	1475(22)	−33(5)	9228(10)
C(46)	971(13)	170(4)	8369(7)
C(51)	4154(9)	1254(3)	3472(5)
C(52)	4931(15)	1602(5)	2960(7)
C(53)	5600(19)	1426(6)	2195(8)
C(54)	5607(16)	902(6)	1973(7)
C(55)	4856(24)	558(5)	2460(9)
C(56)	4177(19)	725(4)	3228(8)
C(61)	2493(11)	2865(3)	5118(5)
C(62)	4006(12)	2845(4)	5582(6)
C(63)	5158(15)	3215(5)	5347(9)
C(64)	4825(20)	3577(5)	4684(9)
C(65)	3362(20)	3592(5)	4222(8)
C(66)	2194(16)	3243(4)	4439(7)
C(11)	2899(12)	292(4)	5308(6)
O(11)	2880(11)	−141(3)	5048(6)
C(12)	4959(11)	855(3)	6399(6)
O(12)	6188(9)	784(3)	6777(5)
C(21)	1883(11)	2060(3)	7675(6)
O(21)	2410(10)	2228(3)	8363(5)
C(22)	−1011(11)	1915(4)	6867(6)
O(22)	−2255(8)	2011(3)	7056(5)
C(31)	332(11)	1932(5)	3394(7)
O(31)	308(11)	2157(4)	2718(6)
C(32)	201(12)	860(4)	4088(8)
O(32)	−84(12)	459(3)	3768(7)
C(33)	−1602(11)	1634(5)	4859(7)
O(33)	−2905(7)	1668(4)	5004(6)

X-ray structure determinations

Suitable crystals of the compounds $[Ru_3(\mu\text{-}H)_2(\mu_3\text{-}PPh)(PH_2Ph)(CO)_8]$, $[Ru_3(\mu\text{-}H)(\mu\text{-}PHPh)_3(CO)_7]$ and $[Ru_6(\mu\text{-}H)_2(\mu_4\text{-}PPh)_2(\mu_3\text{-}PPh)_2(CO)_{12}]$ were each obtained by slow evaporation of hexane–dichloromethane mixtures. The crystals obtained for the hexanuclear compound were the least satisfactory and this limited the quality of the structure determination. Crystal data for these three compounds and basic information on data collection, structure solution and refinement are given in Table 6 while fractional atomic coordinates are given in Tables 7, 8 and 9, respectively. In each case cell dimensions were obtained from the number of orientation reflections given which were selected from a rotation photograph. The intensities of three standard reflections were measured periodically throughout the data collections and the data set cor-

TABLE 9. Fractional atomic coordinates ($\times 10^4$) for the cluster $[Ru_6H_2(PPh)_4(CO)_{12}]$

	x	y	z
Ru(1)	5106(3)	6879(2)	3278(1)
Ru(2)	5548(3)	8067(2)	1842(2)
Ru(3)	4545(3)	6168(2)	1944(1)
Ru(4)	2175(3)	8612(2)	3679(1)
Ru(5)	2522(3)	9686(2)	2207(1)
Ru(6)	1323(3)	7867(2)	2424(1)
P(1)	551(8)	9606(7)	3033(5)
P(2)	6622(8)	6320(7)	2151(5)
P(3)	3460(9)	7994(7)	1525(5)
P(4)	2928(8)	6739(6)	3179(4)
C(71)	−1143(43)	10505(36)	3297(22)
C(72)	−2308(42)	10251(36)	3752(22)
C(73)	−3671(44)	10928(35)	4000(23)
C(74)	−3966(45)	11870(36)	3649(22)
C(75)	−2952(42)	12247(36)	3183(22)
C(76)	−1526(43)	11549(35)	2986(22)
C(81)	8375(43)	5354(36)	1866(23)
C(82)	8922(43)	4470(35)	2249(23)
C(83)	10273(43)	3639(36)	1991(22)
C(84)	11088(45)	3891(35)	1373(22)
C(85)	10679(43)	4886(35)	949(23)
C(86)	9254(42)	5548(36)	1217(22)
C(91)	3337(43)	8046(36)	554(23)
C(92)	2776(42)	7265(36)	206(23)
C(93)	2735(42)	7427(36)	−529(23)
C(94)	2930(42)	8238(35)	−933(24)
C(95)	3752(42)	8885(36)	−682(23)
C(96)	3783(42)	8846(36)	54(22)
C(101)	2382(43)	5636(35)	3685(23)
C(102)	1850(42)	4818(34)	3322(23)
C(103)	1401(42)	4081(35)	3815(23)
C(104)	1523(42)	3944(35)	4519(23)
C(105)	1965(41)	4610(35)	4888(24)
C(106)	2396(7)	5540(6)	4443(4)
C(11)	5739(41)	7621(34)	3921(22)
O(11)	6206(30)	8098(25)	4344(16)
C(12)	5448(41)	5585(34)	3813(21)
O(12)	5773(30)	4725(25)	4141(16)
C(21)	6304(41)	9053(34)	2128(21)
O(21)	6944(30)	9694(25)	2265(16)
C(22)	6535(40)	8046(33)	798(22)
O(22)	6959(30)	8004(25)	185(16)
C(31)	4496(41)	4646(35)	2109(21)
O(31)	4678(30)	3744(26)	2167(16)
C(32)	5387(41)	5774(34)	933(22)
O(32)	5917(30)	5483(25)	332(16)
C(41)	1080(41)	8301(33)	4558(22)
O(41)	251(30)	8077(25)	5093(16)
C(42)	2542(41)	9763(34)	4179(22)
O(42)	2892(30)	10373(25)	4465(16)
C(51)	1742(41)	10504(34)	1430(21)
O(51)	1086(30)	10942(26)	1010(16)
C(52)	3142(41)	10889(34)	2402(21)
O(52)	3496(30)	11640(26)	2586(16)
C(61)	378(41)	8150(34)	1665(22)
O(61)	−452(30)	8395(25)	1178(16)
C(62)	88(43)	7171(33)	2940(21)
O(62)	−1020(31)	6973(25)	3255(16)

rected accordingly. Reflection intensities were corrected for Lorentz and polarisation effects and for absorption by the azimuthal scan method.

The structures were determined by direct methods in each case in the space groups given in Table 6 and the structures refined by alternating cycles of full-matrix least-squares and by difference Fourier synthesis.

For $[Ru_3(\mu\text{-}H)_2(\mu_3\text{-}PPh)(PH_2Ph)(CO)_8]$ all non-hydrogen atoms were refined anisotropically (Table 7). The hydrogen atoms appeared in the difference map but these were included in idealised positions in the Ph rings riding on the carbon atoms with C–H 0.96 Å and $U_{iso} = 0.080$ Å^2. The positions of the hydrogen atoms on the Ru and P atoms were fixed in the final least-squares cycles. The molecule contains a crystallographic mirror plane through Ru(1), P(1), P(2), C(41), C(44), C(51) and C(54).

Likewise for $[Ru_3(\mu\text{-}H)(\mu\text{-}PHPh)_3(CO)_7]$ all non-hydrogen atoms were refined anisotropically and the hydrogen atoms on the phenyl rings were included in idealised positions as above (Table 8). Other hydrogen atoms were not included.

The structure of $[Ru_6H_2(PPh)_4(CO)_{12}]$ was refined with only the Ru and P atoms anisotropic (Table 9). Hydrogen atoms of the phenyl rings were included in idealised positions as above. The Ru-bonded hydrogen atoms were not included.

Calculations were carried out using SHELXTL-PLUS [13] on a MicroVax II computer.

Supplementary material

Tables of thermal parameters, H-atom coordinates, full sets of bond lengths and angles, and tables of observed and calculated structure factors are available from the authors on request.

Acknowledgements

We thank the SERC for research studentships (for S.D. and N.I.P.) and for support for the diffractometer, and Johnson-Matthey for a loan of ruthenium trichloride.

References

1 F. Iwasaki, M. J. Mays, P. R. Raithby, P. L. Taylor and P. J. Wheatley, *J. Organomet. Chem., 213* (1981) 185.

2 K. Natarajan, L. Zsolnai and G. Huttner, *J. Organomet. Chem., 220* (1981) 365.

3 C. Choo Yin and A. J. Deeming, *J. Chem. Soc., Dalton Trans.*, (1973) 1013.

4 K. A. Azam, A. J. Deeming, I. P. Rothwell, M. B. Hursthouse and J. D. J. Backer-Dirks, *J. Chem. Soc., Dalton Trans.*, (1981) 2039.

5 J. S. Field, R. J. Haines and D. N. Smit, *J. Organomet. Chem., 224* (1982) C49.

6 J. S. Field, R. J. Haines and D. N. Smit, *J. Chem. Soc., Dalton Trans.,* (1988) 1315.

7 L. M. Bullock, J. S. Field, R. J. Haines, E. Minshall, M. H. Moore, F. Mulla, D. N. Smit and L. M. Steer, *J. Organomet. Chem., 381* (1990) 429.

8 J. S. Field, R. J. Haines and F. Mulla, *J. Organomet. Chem., 389* (1990) 227.

9 R. P. Rosen, G. L. Geoffroy, C. Bueno, M. R. Churchill and R. B. Ortega, *J. Organomet. Chem., 254* (1983) 89.

10 V. D. Patel, A. A. Cherkas, D. Nucciarone, N. J. Taylor and A. J. Carty, *Organometallics, 4* (1985) 1792.

11 A. M. Arif, T. A. Bright, D. E. Heaton, R. A. Jones and C. M. Nunn, *Polyhedron, 9* (1990) 1573.

12 A. M. Arif, T. A. Bright, R. A. Jones and C. M. Nunn, *J. Am. Chem. Soc., 110* (1988) 6894.

13 G. M. Sheldrick, *SHELXTL-PLUS,* an integrated system for refining and displaying crystal structures from diffraction data, University of Göttingen, FRG, 1986.